Effects of Different Shot Peening Treatments in Combination with a Superfinishing Process on the Surface Durability of Case-Hardened Gears

Dominik Kratzer, Johannes König, Thomas Tobie and Karsten Stahl

Introduction

Increasing demands on power transmission and reduction in mass of modern gearboxes lead to gear designs that are close to their load-carrying capacity limits. Therefore, the probability of different failure modes like pitting, scuffing and wear increases if there are no improvements in surface durability. Possible measures to strengthen the gear's flank load-carrying capacity include shot peening and superfinishing. During the shot peening process, compressive residual stresses are induced in the surface near area of the gear (Ref. 5). According to König et al. (Ref. 11), this can lead to a significant increase in pitting resistance. Another possibility to strengthen a gear's surface is to reduce its surface roughness, for example, with superfinishing processes. Both positive effects have been proven in multiple experimental research projects (Refs. 10, 11, 15 and 17), but the combined applicability in a predictive surface durability calculation has not been proven until now. This paper presents the results of these investigations, which were carried out as a part of the FVA (Research Association for Drive Technology) research project 521 II (Ref. 12).

State of the Art and Research Objectives

The scientific literature (Refs. 10–11; 15 and 17) contains numerous investigations describing the influence of smooth surfaces due to superfinishing processes and residual stresses on the surface durability of gears. Schwienbacher et al. (Ref. 13) and König et al. (Ref. 11) proposed an extension of the calculation approach described in ISO 6336-2 (Ref. 9) to consider these effects.

According to the international gear rating standard ISO 6336-2 (Ref. 9), the permissible contact stress for gears is calculated using Equation 1:

$$\sigma_{HP} = \frac{\sigma_{Hlim} \cdot Z_{NT}}{S_{Hmin}} Z_L \cdot Z_v \cdot Z_R \cdot Z_W \cdot Z_X \quad (1)$$

Where

σ_{HP} is Permissible contact stress
σ_{Hlim} is Allowable stress number for contact stress
S_{Hmin} is Minimum required safety factor for surface durability
Z_{NT} is Life factor
Z_L is Lubricant factor
Z_v is Velocity factor
Z_R is Roughness factor
Z_W is Work hardening factor
Z_X is Size factor

Schwienbacher et al. (Ref. 13) investigated the influence of grinding temper on the flank load-carrying capacity of case-hardened gears. As a result, grinding temper caused reduced hardness depth profile values and reduced compressive residual stress profile values (Ref. 6). These effects were considered to be responsible for the resulting reduced surface durability.

Subsequently the calculation according to ISO 6336-2 (Ref. 9) was extended using the proposed surface factor Z_S to take these effects into consideration. Moreover, the investigations by König et al. (Ref. 11) showed that smoother flank surfaces lead to a higher pitting load-carrying capacity. In order to take this effect into consideration in the calculation model for the endurance strength in ISO 6336-2 (Ref. 9), the Z_R factor was replaced by the factor $Z_{R,GS}$. The resulting calculation approach for the permissible contact stress is shown in Equation 2.

$$\sigma_{HP} = \frac{\sigma_{HLIM} \cdot Z_{NT}}{S_{Hmin}} Z_L \cdot Z_v \cdot Z_{R,GS} \cdot Z_W \cdot Z_X \cdot Z_S \quad (2)$$

Where

$Z_{R,GS}$ is Roughness factor for superfinished gears
Z_S is Surface factor

Detailed descriptions of the calculation approaches for the factors Z_S and $Z_{R,GS}$ are presented in the following.

Calculation of Z_S

Schwienbacher et al. (Ref. 13) detected that the flank load-carrying capacity of case-hardened gears is influenced by the degree of grinding temper on the gears' flanks. The reduced compressive residual stresses and reduced hardness value in surface near material regions due to grinding temper were considered as the main reason for the reduced flank load-carrying capacity compared to gears without grinding temper. Therefore Schwienbacher et al. (Ref. 13) correlated the resulting flank load-carrying capacity of gear batches with different degrees of grinding temper with the measurement results for the residual stress depth profile and the hardness depth profile. As a result the surface factor Z_S according to Equation 3 consists of a factor regarding the influence of hardness ($Z_{S,HV}$) and a factor regarding the influence of the residual stresses ($Z_{S,ES}$) according to Equations 4–5 and as defined by Schwienbacher et al. (Ref. 13).

$$Z_S = Z_{S,HV}^{0.49} \cdot Z_{S,ES}^{0.51} \quad (3)$$

$$Z_{S,HV} = 1 + \frac{1.68 \cdot \overline{\Delta HV_{int\_xn}}}{621\,HV1} \text{ with } \overline{\Delta HV_{int\_xn}} = \overline{HV_{int\_xn}} - \overline{HV_{int\_xn\_Ref}} \quad (4)$$

$$Z_{S,ES} = 1 + \frac{1.91 \cdot \overline{\Delta ES_{int\_xn}}}{6575\,N/mm^2} \text{ with } \overline{\Delta ES_{int\_xn}} = \overline{ES_{int\_xn}} - \overline{ES_{int\_xn\_Ref}} \quad (5)$$

Where

$Z_{S,HV}$ is Surface hardness factor

$Z_{S,ES}$ is Surface residual stress factor

$\overline{\Delta HV_{int\_xn}}$ is Difference of the integral hardness value up to the depth x_n compared to a reference batch, HV1

$\overline{\Delta ES_{int\_xn}}$ is Difference of the integral residual stress value up to the depth x_n compared to a reference batch, N/mm²

$\overline{HV_{int\_xn}}$ is Integral hardness value up to the depth x_n , HV1

$\overline{HV_{int\_xn\_Ref}}$ is Integral hardness value of the reference batch up to the depth x_n, HV1

$\overline{ES_{int\_xn}}$ is Integral residual stress value up to the depth x_n, N/mm²

$\overline{ES_{int\_xn\_Ref}}$ is Integral residual stress value of the reference batch up to the depth x_n , N/mm²

Since the factor Z_S takes into account deviations in comparison to a reference, the $\overline{\Delta HV_{int\_xn}}$ and $\overline{\Delta ES_{int\_xn}}$ values are calculated by comparing the investigated gear batch ($\overline{HV_{int\_xn\_Ref}}/\overline{ES_{int\_xn\_Ref}}$) with a known reference batch ($\overline{HV_{int\_xn\_Ref}}/\overline{ES_{int\_xn\_Ref}}$). The variables $\overline{\Delta HV_{int\_xn}}$ and $\overline{\Delta ES_{int\_xn}}$ in Equations 4–5 are obtained by numerically integrating the subsurface measuring points up to the depth x_n. The depth x_n is the minimum depth from the surface at which the hardness or residual stress profile of the investigated gear batch deviates from the reference gear batch. The variables are calculated as described in Equations 6 and 7.

$$\overline{HV_{int\_xn}} = \frac{1}{x_n} \cdot \sum_{i=1}^{n-1} \frac{HV_{i+1} + HV_i}{2} \cdot (x_{i+1} - x_i) \tag{6}$$

$$\overline{ES_{int\_xn}} = \frac{1}{x_n} \cdot \sum_{i=1}^{n-1} \frac{\sigma_{E_{i+1}} + \sigma_{E_i}}{2} \cdot (x_{i+1} - x_i) \tag{7}$$

Where

x_i is Depth of measurement point i, mm

HV_i is Surface hardness at measurement point i, HV1

σ_{E_i} is Residual stress value at measurement point i, N/mm²

Calculation of $Z_{R,GS}$

König et al. (Ref. 11) investigated gears which were subjected to a shot peening and a superfinishing process. Shot peening leads to increased subsurface compressive residual stress values, which might affect the surface durability (Ref. 5). To take this effect into consideration when calculating the pitting load-carrying capacity, König et al. (Ref. 11) used the above mentioned approach according to Schwienbacher et al. (Ref 13). It was shown that the calculation results show a good correlation with the experimental results. Since only a limited number of gear variants were investigated, different peening conditions still had to be validated.

Since an additional superfinishing process was applied to all gear batches investigated by König et al. (Ref. 11), a significant refinement of the surface roughness values compared to the conventionally ground gear batch occurred in accordance with other research (Refs. 16–17). The influence of the surface roughness on the pitting load-carrying capacity is regarded in the rating method according to ISO 6336-2 by the surface roughness factor Z_R as defined in Equation 8 for case-hardened gears.

$$Z_R = \left(\frac{3}{Rz_{10}}\right)^{0.08} \tag{8}$$

Where

Z_R is Roughness factor

Rz_{10} is Mean relative peak-to-valley roughness for the gear pair

The Z_R factor according to ISO 6336-2 (Ref. 9) covers values for Rz_{10} down to 1 µm. Since the Rz_{10} values for superfinished gears are below this limit, the possible extension of the given ISO formula was investigated. The experiments by König et al. (Ref. 11) showed that the ISO factor Z_R for superfinished gears might be replaced by the factor $Z_{R,GS}$. The factor can be calculated according to Table 1 or derived graphically (Fig. 1). The factor $Z_{R,GS}$ limits the theoretical curve of Z_R to the value 1.14. The factor $Z_{R,GS}$ of König et al. (Ref. 11) is calculated according to DIN 3990-2 (Ref. 2) and based on the Rz_{100} value. In the following, this factor is replaced by the Rz_{10} value according to the new convention in ISO 6336-2 (Ref. 9).

The limit of 1.14 for the $Z_{R,GS}$ factor results from the experimentally covered range of roughness values. A further extension of applicability of $Z_{R,GS}$ to lower roughness values has not yet been investigated.

In summary, the application of the surface factor Z_S for shot peened gears and the extension of the roughness factor Z_R *to* $Z_{R,GS}$ are possibilities for taking into consideration positive

Table 1 Workflow for determining $Z_{R,GS}$ according to König et al. (Ref. 11)

Step 1: All of the following conditions must be true: 1. Gears are case-hardened 2. Gears are superfinished 3. Safety factor against micropitting of $S_\lambda > 2$	
All are true	Replace Z_R with $Z_{R,GS}$ (proceed to Step 2)
Any is false	Use Z_R according to DIN 3990-2 / ISO 6336-2
Step 2: Check if $\left(\frac{3}{Rz_{100}}\right)^{0.08} > 1.14$	
Is true	$Z_{R,GS} = 1.14$
Is false	$Z_R = \left(\frac{3}{RZ_{100}}\right)^{0.08} > 1.14$

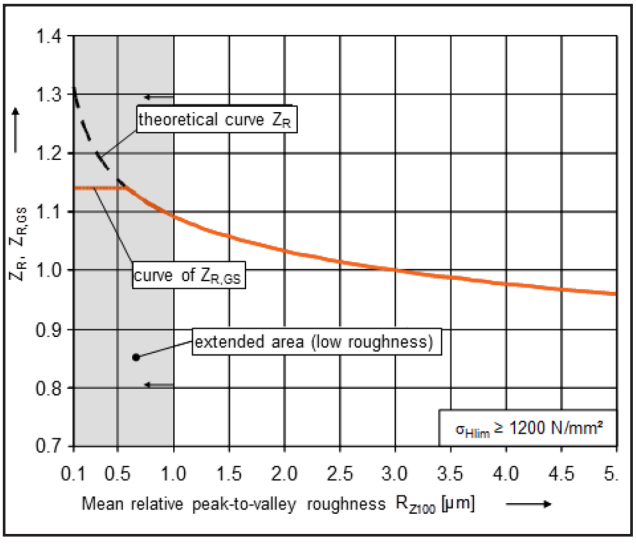

Figure 1 Curve of the roughness factor Z_R and the extension $Z_{R,GS}$ according to König et al. (Ref. 11)

effects of gear surface refinements when calculating the pitting load-carrying capacity of gears. For the surface factor Z_S, a validation for different shot peening processes and the resulting different subsurface compressive residual stress profiles is pending, as well as the validation of the existing calculation approach for the surface roughness factor $Z_{R,GS}$ for even finer surface roughness values. These topics are addressed, evaluated and concluded in the following.

Test Program and Methods

To prove that the surface factor Z_S can be applied to consider the positive effects of increased compressive residual stresses in the flank-load carrying capacity calculation, as well as to validate the applicability of the roughness factor $Z_{R,GS}$ for smoother gear surfaces than investigated by König et al. (Ref. 11), numerous flank load-carrying capacity tests were carried out. For the tests relating to the applicability of the surface factor Z_S in the load area of high cycle fatigue, five variants were tested at the same load level in order to compare the mean load cycles until failure occurs. In order to prove the applicability of the $Z_{R,GS}$ factor for values above 1.14, S-N-curves were evaluated for several variants with different flank roughness values. For the superfinished batches with very smooth surfaces, vibratory finishing with and without chemical enhancement were applied after the conventional grinding to obtain even finer surface roughness values. The shot peening process took place between the grinding and the superfinishing processes. All variants and the intended purpose are summarized in Table 2.

Table 2 Investigated variants and purpose of the corresponding shot peening treatment

	Manufacturing	Purpose
R1	Unpeened reference	Reference
RGS	Shot peened and superfinished	Conventional process parameters
ET1	Shot peened and superfinished	Residual stress profile with same maximum values as RGS but closer to surface
ETT	Shot peened and superfinished	Residual stress profile with higher values into the depth of the material
EB	Shot peened and superfinished	Residual stress profile with reduced maximum value
EV	Shot blasted and superfinished	Residual stress profile after shot blasting
GSL	Shot peened and superfinished	Minimal surface roughness with conventional peening process
02	Superfinished	Minimal surface roughness without additional peening process

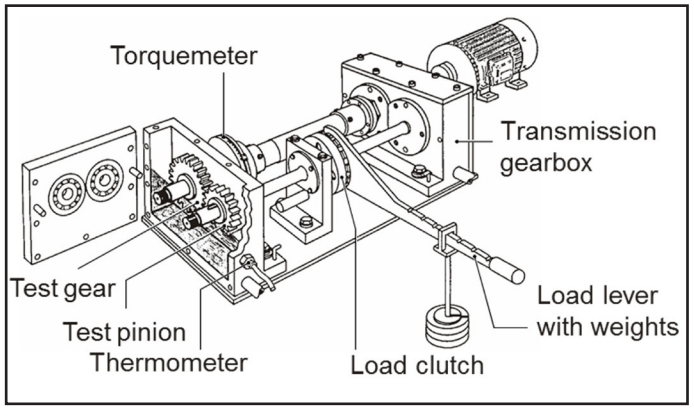

Figure 2 FZG back-to-back gear test rig (Ref. 7).

Table 3 Gear variant

	Symbol	Pinion	Wheel
Material		16MnCr5	
Number of teeth	$z_{1,2}$	17	18
Face width	b	10 mm	
Normal module	m_n	5 mm	
Profile shift coefficient	x	0.514	0.407
Normal pressure angle	α_n	20°	
Helix angle	β	0°	

To validate the calculation model for the roughness factor $Z_{R,GS}$, experimental tests were carried out with a FZG back-to-back gear test rig in accordance with ISO 146351 (Ref. 7) in order to obtain the nominal endurance strength for 50 % failure probability of the variants RGS, ET1, EB, GSL and O2. Generally, the gears in the test and transmission gearboxes are loaded by rotating the two shaft parts next to the load clutch in opposite directions. By locking the load clutch, a closed mechanical power circuit results. The desired pressure on the test gears is monitored by locking the load clutch at certain angles of rotation, depending on the intended amount of load. Controlling this angle of rotation after a defined number of revolutions guarantees the stability of the applied torque. The electric motor drives the test gears at the required pinion speed of 3,000 rpm. The lubricant FVA 3 with 4 % anglamol, a sulfur and phosphorus containing additive, at 60°C by way of injection lubrication was used for the investigations, as there is an extensive data base for this type of oil.

The geometry of the test gear was used in accordance to other research projects at FZG with the aim to investigate the flank load-carrying capacity. The gears' geometry is summarized in Table 3. All gears were manufactured from 16MnCr5, case-hardened, mechanically cleaned by shot blasting and ground. Depending on the variant described in Table 2, the mentioned shot blasting respectively shot peening took place before the final superfinishing process. Details of the corresponding process parameters are described in (Ref. 12). Figure 3 shows sample gear flanks after conventional grinding in the left picture and superfinishing in the right picture.

Gear Documentation

The gear geometry, surface roughness, material characteristics and micro-structure, the hardness profile and residual stress profile were documented before each test.

The gear quality was measured according to DIN 3962 (Ref. 1)

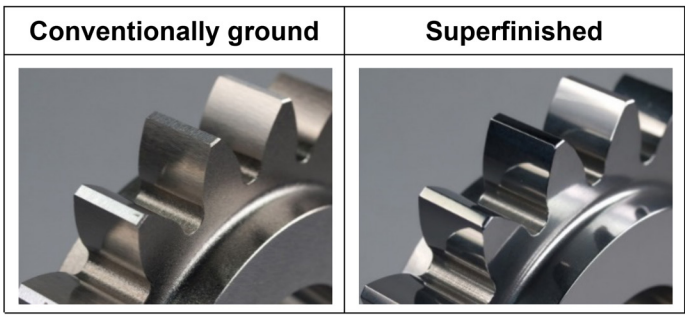

Figure 3 Surface appearance.

Table 4 Roughness measurements		
Gear variant	Ra in µm	Rz in µm
R1	0.34	2.11
RGS	0.12	0.77
ET1	0.15	0.96
ETT	0.06	0.48
EB	0.15	0.99
EV	0.18	1.13
GSL	0.07	0.46
02	0.07	0.39

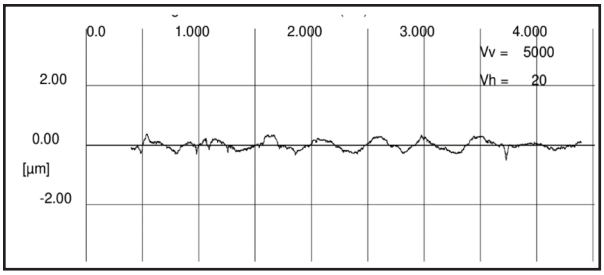

Figure 4 Sample roughness profile of a superfinished gear.

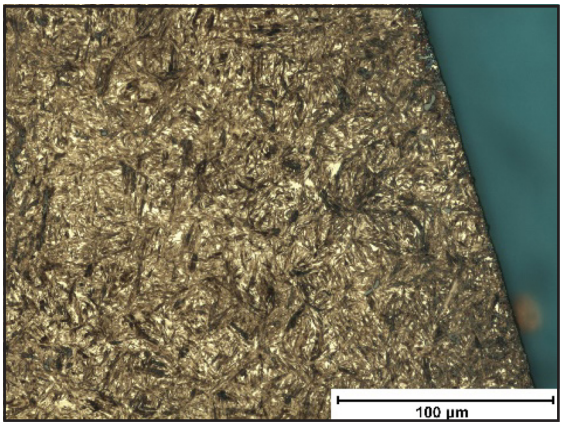

Figure 5 Etched metallographic microsection of a representative test gear.

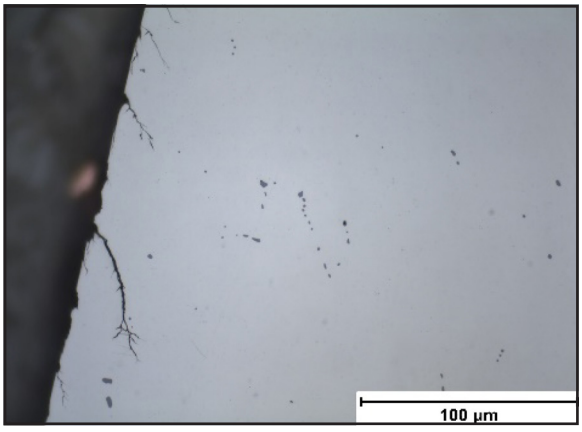

Figure 6 Unetched metallographic microsection of the variant ETT (before any testing).

using a gear measurement center Klingelnberg P40. Three teeth of every gear were measured. All relevant gear quality values were better than quality class 5, which is required for flank load-carrying tests.

The roughness was measured using the Hommel T8000 profilometer with applied high-pass filter according to DIN EN ISO 11562 (Ref. 3). Every gear was measured on three flanks evenly distributed over the circumference. A sample measurement report for a superfinished gear is documented in Figure 4. The average values of the characteristic roughness parameters for the investigated variants are shown in Table 4. Further details as well as determined roughness parameters are documented (Ref. 12).

To evaluate the microstructure of the gear variants, metallographic micro-sections were prepared for each variant. Since all gears were manufactured from the same steel bar and in the same heat treatment batch, all the gears should have the same microstructure. The typical microstructure in Figure 5 shows martensitic structure near the surface with a limited amount of retained austenite, typical for case-hardened gears. As a result, all variants fulfilled the requirements for the MQ material quality class as specified in ISO 6336-5 (Ref. 8). Thus, the microstructure is unlikely to have a negative impact on the pitting load-carrying capacity. Some undesired effects were only detected for the ETT variant. Obviously, the very intensive shot peening process resulted in small cracks on the surface before any testing was done, which can be seen in Figure 6. These small cracks are unusual for case-hardened and ground gears and therefore might influence the surface durability of this test series, as discussed later in this paper.

The hardness profile was measured for every investigated variant. Since the heat treatment was performed in one batch

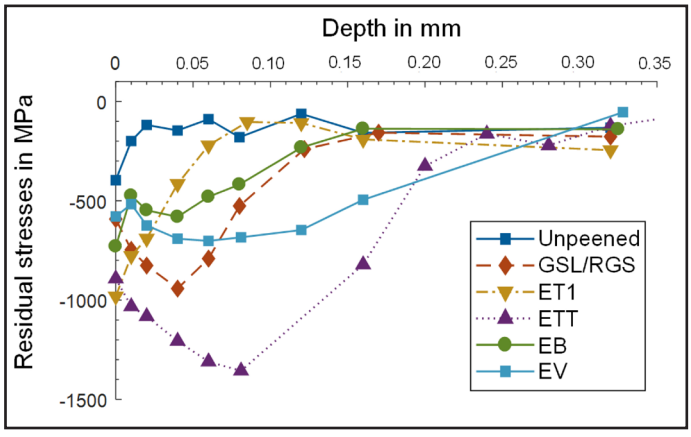

Figure 7 Residual stress profiles, measured by x-ray diffraction at the gear flank of the different test series in new condition.

for all investigated gears, the hardness depth profiles were close to identical for all variants. Surface hardness, core hardness and CHD-values corresponded to the specifications of ISO 6336-5 (Ref. 8). Therefore, the influence of the hardness on the Z_S factor mentioned previously in Section 2 can be neglected for the test series investigated here.

The residual stresses were measured using a Seifert XRD 3003 PTS x-ray diffractometer by repeatedly measuring and removing the surface layer with acid to obtain information about the depth of the material. The measurement parameters are documented in detail in (Ref. 12). The measurement results are presented (Fig. 7). As intended, the variants show different residual stress depth profiles depending on the applied shot peening treatment. It can be noted that the measurement results correspond with the intended purpose described in Table 2.

Calculation Results

To investigate if the experimental results are adequately represented by the previous calculation approaches in Section 2 the factors Z_S an $Z_{R,GS}$ have to be calculated for every gear variant. Therefore the measurement results in section 4 are utilized.

The surface factor Z_S can be calculated according to Equation 3 with the results of the hardness and residual stress measurements. As already mentioned, the hardness depth profiles do not differ significantly for any variant, and therefore the $Z_{S,HV}$ factor can be set equal to one for all test series investigated here. As a result, the surface factor Z_S is solely influenced by the residual stress depth profile. The calculation according to the previous section results in the values shown in Table 5.

Table 5 also shows the results of the roughness factor $Z_{R,GS}$ calculation based on the measured roughness values taken from Table 4. The applicability of the calculation results for $Z_{R,GS}$ with values up to 1.14 has been scientifically proven by König et al. (Ref. 11), based on the calculation approach in ISO 6336 (Ref. 9). Values for $Z_{R,GS}$ above 1.14 for even smoother gear flanks have not been investigated until now.

Since the remaining boundary conditions influencing the factors besides Z_S and $Z_{R,GS}$ in Equation 2 are kept the same by the manufacturing and test process, the product $Z_S \cdot Z_{R,GS}$ (Table 5) represents the theoretical expectation for the resulting pitting durability. The applicability of the calculation model will be verified by experimental investigations in the following.

Table 5 Calculated surface and roughness factors according to Section 2 for the investigated test series

Gear variant	Z_s	$Z_{R,GS}$	$Z_s \cdot Z_{R,GS}$
RGS	1.07	1.10	1.18
ET1	1.06	1.10	1.16
ETT	1.12	1.16	1.30
EB	1.05	1.09	1.14
EV	1.07	1.08	1.16
GSL	1.07	1.16	1.24
02	1.0	1.17	1.17

Table 6 Experimental results for the pitting load-carrying capacity (1) – not investigated)

Variant	Mean load cycles at σ_{H0} = 1750 N/mm²	$\sigma_{H0\infty,50\%}$ in N/mm²
RGS	62 million	1701
ET1	21 million	1716
ETT	48 million	1)
EB	21 million	1542
EV	24 million	1)
GSL	1)	1877
02	1)	1746

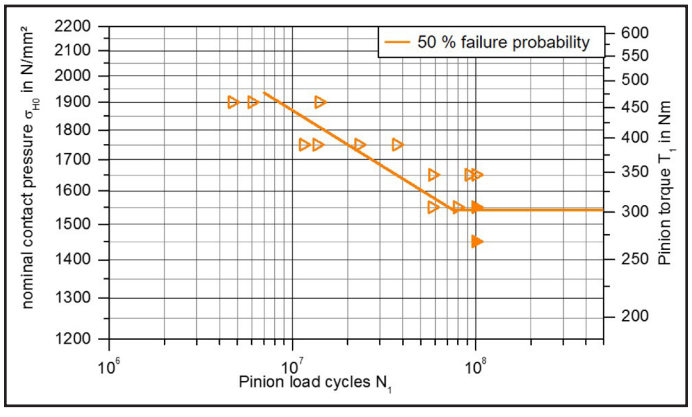

Figure 8 S-N-curve of the variant EB.

Experimental Results

To obtain the pitting load-carrying capacity of the investigated gear variants, tests using the FZG back-to-back test rig were carried out at different load stages. To determine the S-N-curve, load stages in the regime of high cycle fatigue and fatigue limit were investigated. Figure 8 shows by way of example the test results for the variant EB in the double logarithmic diagram as triangular markers. Test runs that reached the limit of 100 million load cycles without pitting are shown with solid markers. The tests were performed according to the FVA directive 563 I (Ref. 14). For the following evaluations, the sustained mean load cycles at a nominal contact pressure of σ_{H0} = 1750 N/mm² as well as the nominal endurance strength for failure probability of 50 % ($\sigma_{H0\infty,50\%}$) are summarized (Table 6).

To investigate whether the reported reduction in micropitting appearance with finer surface roughness of the gear flank can be reproduced in the current scope of experiments, sampling tests were carried out with a reference variant R1 that was manufactured using a conventional grinding process. The mean roughness value Ra was equal to 0.34 µm for this variant. During test runs with such gears, micropitting occurred over major parts of the gear flank starting in the area of negative sliding below the pitch circle, as can be seen in Figure 9. Figure 10 shows a typical superfinished gear flank with scratch marks due to the initial tooth contact after a test run. While most of the superfinished gears only show micropittings as consequential damage around

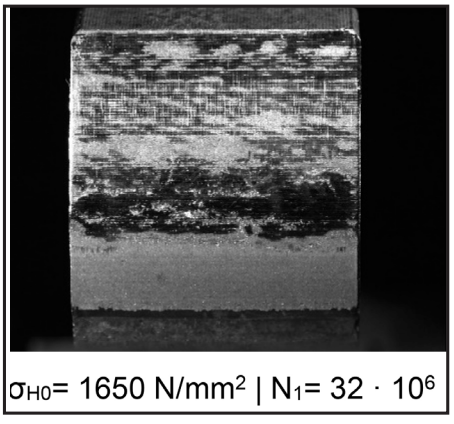

Figure 9 R1 flank surface after test.

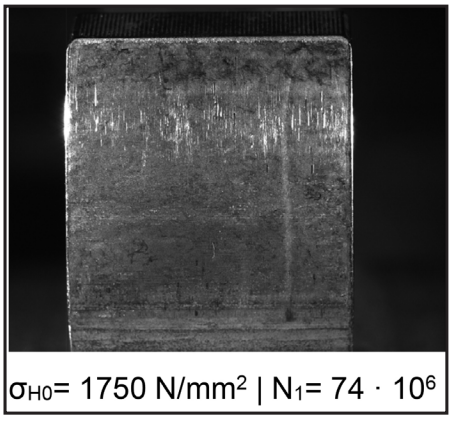

Figure 10 RGS flank surface after test.

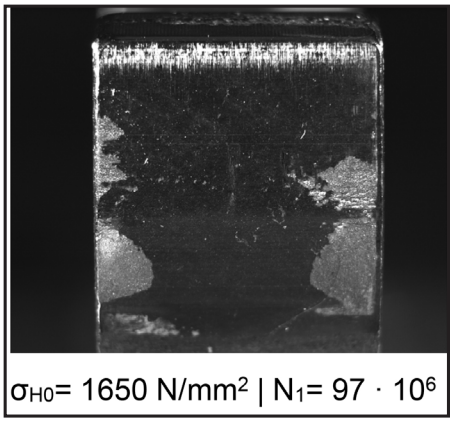

Figure 11 EB flank surface after test.

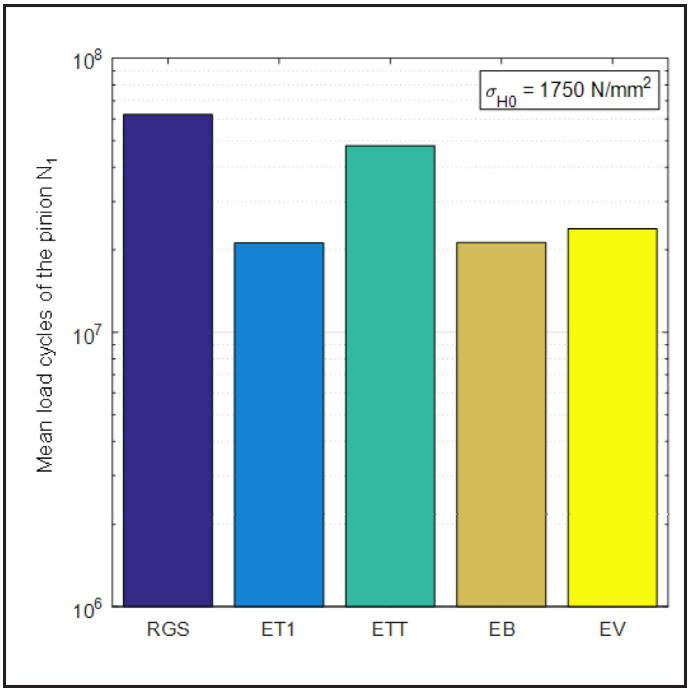

Figure 12 Mean load cycles until failure base on the test results at σ_{H0} = 1750 N/mm².

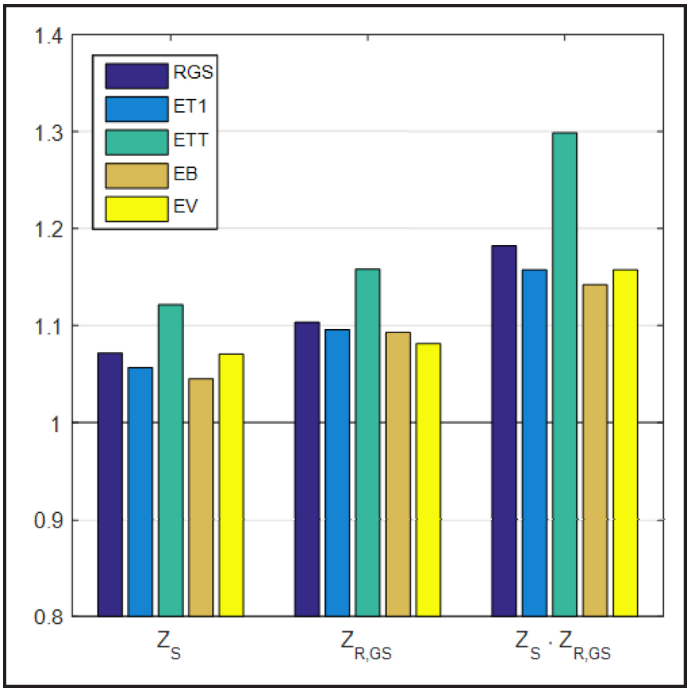

Figure 13 Calculated factors Z_S, $Z_{R,GS}$ and the resulting product.

damaged flank regions due to the locally increased stress, the variant EB shows micropittings extending from the sides of the flanks. This could be due to manufacturing deviations, which lead to local bulges on the flank sides.

In summary the results confirm the effects described in literature (Refs. 16–17) concerning the significant reduction of micropitting occurrence if smooth surfaces without local geometric deviations are guaranteed.

Evaluation of Results

Variation in residual stress profile. To determine whether the $Z_{R,GS}$ and Z_S factors can be used to qualitatively compare the mean load cycles until failure in the load region of high cycle fatigue, FZG back-to-back test rig tests were evaluated at the nominal contact stress of 1750 N/mm² for the variants RGS, ET1, ETT, EB and EV. For each variant, the resulting mean load cycles at that stress level and the calculated factors Z_S, $Z_{R,GS}$ as well as the product $Z_S \cdot Z_{R,GS}$ are summarized in Table 5 and Table 6. Figure 12 shows the resulting mean load cycles in a logarithmically scaled bar graph, while Figure 13 shows bar graphs of the calculated factors.

It is noticeable that the calculated factors for the ETT variant obtain high values due to the distinct compressive residual stress profile and the very fine surface roughness. In contrast to the resulting theoretical expectation, the ETT variant achieved less load cycles in the test runs than the RGS variant. This might be due to the small surface cracks shown (Fig. 6), which were caused during the manufacturing process. Therefore, the application of the surface and roughness factor in the pitting lifetime prediction is limited to manufacturing processes, which do not cause surface cracks.

The remaining variants RGS, ET1, EB and EV demonstrate a good correspondence between the test results in Figure 12 and the expectations based on the calculated factors (Fig. 13). The higher number of mean load cycles of the RGS variant is well represented by the higher value of the product $Z_S \cdot Z_{R,GS}$. The remaining variants ET1, EB and EV have similar mean load cycles, while the product of the factors has a slightly lower value for the EB variant. Since the Z_S factor was originally created to calculate the nominal endurance strength, such deviations were expected for a comparison of the mean load cycles in the load region of high cycle fatigue. Nevertheless, it was proven that the product of Z_S and $Z_{R,GS}$ can be applied to qualitatively compare the expecTable mean load cycles if the shot peening process does not result in a damaged gear surface.

Allowable stress number. Since all the investigated gears were manufactured from one material and in one heat-treatment batch, the allowable pitting stress number σ_{Hlim} should be similar. By applying the calculation approach based on ISO 6336-2 (Ref. 9), however, the results $\sigma_{Hlim,ISO6336}$ show distinct deviations (Table 7). This is due to the insufficient consideration of the compressive residual stress state and surface roughness for shot peened and superfinished gears in the current ISO standard. Therefore, the aforementioned factors $Z_{R,GS}$ and Z_S were applied. By considering these factors in the calculation of σ_{Hlim}, a significant reduction in the scattering of the results can be observed for the investigated variants. For these allowable stress numbers, labeled with $\sigma_{Hlim,experiment}$ (Table 7), only the EB variant shows a larger deviation. Some gear flanks of the EB variant showed micropittings extending from the sides of the flank as shown (Fig. 11). According to Felbermaier et al. (Ref. 4), micropittings,

Table 7 Experimental results

Variant	$\sigma_{H0\infty,50\%}$	$\sigma_{Hlim,ISO6336}$	$\sigma_{Hlim,experiment}$
RGS	1701 N/mm²	1701 N/mm²	1583 N/mm²
ET1	1716 N/mm²	1723 N/mm²	1631 N/mm²
EB	1542 N/mm²	1552 N/mm²	1484 N/mm²
GSL	1877 N/mm²	1877 N/mm²	1656 N/mm²
02	1746 N/mm²	1746 N/mm²	1631 N/mm²

which arise during the tests, might reduce the pitting load-carrying capacity by about 7%. Taking this into account, the calculated allowable stress number for the EB variant aligns with the other test results. Since the results for the variants RGS, ET1, GSL and O2 also match well, it is assumed that the effects of the peening and superfinishing processes are adequately represented by the extended calculation factors.

Extension of $Z_{R,GS}$ factor. For the extension of the upper limit for $Z_{R,GS}$, S-N-curves were determined for the variants GSL and O2. The gears of the GSL variant were shot-peened in accordance with the state of the art and then superfinished. The average surface roughness after superfinishing was $Rz = 0.46$ µm, which results in a roughness factor of 1.16 according to the theoretical Z_R curve. A roughness factor of 1.17 was calculated for the variant O2. The classification of the test results with the allowable stress number according to the ISO standard, carried out in section 7.2, shows that the application of the increased roughness factor correctly reflects the obtained test results, independent of any previously applied shot peening. For the increased roughness factor, a new limit value of $Z_{R,GS,max} = 1.17$ can therefore be applied on the basis of the documented test results. $Z_{R,GS}$ is on the slightly conservative side, especially for variants with the finest surface roughness values. The scatter range already existing in the ISO standard can also be applied therefore to the newly set limit value. However, this range should not be used without further experimental verification. Following the approach of König et al. (Ref. 11) the upper limit for $Z_{R,GS}$ in Table 1 can be set to 1.17 and the graph for the roughness factor can be extended as shown in Figure 14.

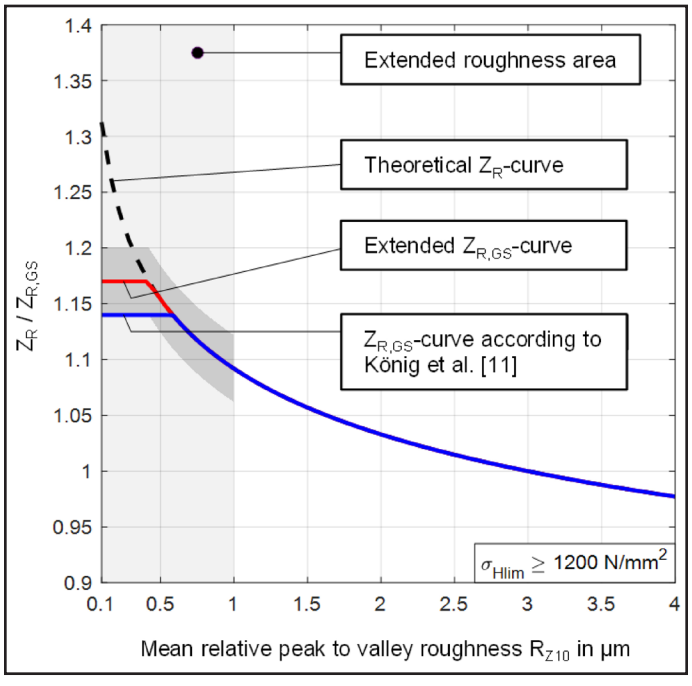

Figure 14 Curves of the roughness factor Z_R and the extension $Z_{R,GS}$.

Conclusion

An extensive experimental study with differently shot peened and superfinished gears was carried out in order to investigate the applicability of the proposed surface factor Z_S for different residual stress profiles and to extend the scope of application for the roughness factor $Z_{R,GS}$.

Superfinished variants showed significantly less micropitting appearance after testing compared to the conventionally ground variant. As root cause for this effect it is presumed that the superfinished flank surfaces are smooth and without bulges. If bulges are present, they may lead to a locally increased stress, which results in a higher probability of micropitting.

In order to investigate the resulting mean load cycles until failure, numerous variants, which underwent different shot peening processes and therefore showed different subsurface compressive residual stress profiles, were tested at the same load level in the region of high cycle fatigue. It was possible to show, that the factors Z_S and $Z_{R,GS}$ can be applied to qualitatively compare the different variants, provided that no surface damage was caused by the shot peening treatment.

So far the calculation approach according to ISO 6336 (Ref. 9) is based on investigations with conventionally manufactured, ground gears. Gears with increased compressive residual stresses due to shot peening processes and smooth surfaces due to superfinishing processes are not considered yet. By extending the ISO 6336 (Ref. 9) calculation approach by the Z_S factor as well as the $Z_{R,GS}$ factor according to König et al. (Ref. 11) a good correlation results for the calculated allowable stress numbers. Therefore, it is assumed that the factor Z_S and $Z_{R,GS}$ are suiTable to take the positive effects of different shot peening processes as well as superfinishing processes into account for gearbox design and rating processes. Furthermore the roughness factor for superfinished gears $Z_{R,GS}$ can be applied to higher values than suggested by König et al. (Ref. 11). The new maximum value for $Z_{R,GS}$ resulting from the surface roughness of the investigated gears is 1.17.

In summary, shot peening and superfinishing processes can increase the surface durability of case hardened gears significantly. To obtain the optimal effect, the superfinished gear surface must be smooth without bulged flanks and without prior damage originating from the shot peening process.

Acknowledgement. The presented results are based on the research projects IGF no. 14908 N and IGF no. 17145 N undertaken by the Research Association for Drive Technology e.V. (FVA); supported partly by the FVA, the Stiftung Stahlanwendungsforschung im Stifterverband für die Deutsche Wissenschaft e.V. (AVIF) and through the German Federation of Industrial Research Associations e.V. (AiF) in the framework of the Industrial Collective Research Programme (IGF) by the Federal Ministry for Economic Affairs and Energy (BMWi) based on a decision taken by the German Bundestag. The authors would like to thank for the sponsorship and support received from the FVA, AVIF, AiF and the members of the project committee.

For more information.
Questions or comments regarding this paper? Contact Dominik Kratzer at *kratzer@fzg.mw.tum.de.*

References

1. Deutsches Institut für Normung e.V., 1978, "Tolerances for Cylindrical Gears, Part 1 to 3 (in German)", Norm DIN 3962. Beuth Verlag, Berlin.
2. Deutsches Institut für Normung e.V., 1987, "Calculation of load capacity of cylindrical gears - Part 2: calculation of pitting resistance (in German)", Norm DIN 3990-2. Beuth Verlag, Berlin.
3. Deutsches Institut für Normung e.V., 1998, "Surface texture: Profile method - Metrological characteristics of phase correct filters (in German)", Norm DIN EN ISO 11562. Beuth Verlag, Berlin.
4. Felbermaier, M., Tobie, T., and Stahl, K., 2014, „Micropitting - Pitting II". Influence of micropitting on the pitting durability of case-hardened gears in the regime of high cycle fatigue and fatigue limit (in German)" ,Project Nr. 459 II (IGF-Nr. 16088 N), Final report, FVA magazine Nr. 1087, Frankfurt am Main.
5. Güntner, C., T. Tobie and K. Stahl, K. 2017, "Influence of the Residual Stress condition on the Load Carrying Capacity of Case Hardened Gears," American Gear Manufacturers Association, AGMA Technical Paper, 17FTM20.
6. Höhn, B.-R., Stahl, K., Oster, P., Tobie, T., Schwienbacher, S., and Koller, P., 2012, "Grinding Burn on Gears - Correlation between Flank-Load Carrying Capacity and Material Characteristics", The 4th International Conference on Power Transmission, pp.113–123
7. International Organization for Standardization, 2000, "Gears - FZG test procedures - Part 1: FZG test method A/8,3/90 for relative scuffing load-carrying capacity of oils", Norm ISO 14635-1
8. International Organization for Standardization, 2003, "Calculation of load capacity of spur and helical gears – Part 5: Strength and quality of materials", Norm ISO 6336-5:2003(E). Beuth Verlag, Berlin
9. International Organization for Standardization, 2006, "Calculation of load capacity of spur and helical gears – Part 2: Calculation of surface durability (pitting)", Norm ISO 6336-2:2006(E). Beuth Verlag, Berlin
10. Kobayashi, M. and K. Hasegawa. 1990, "Effect of Shot Peening on the Pitting Fatigue *Strength of Carburized Gears*," *Proceedings of the IV International Conference on Shot* Peening,, pp.465–476
11. König, J., P. Koller, T. Tobie and K. Stahl. 2015, "Correlation of Relevant Case Properties and the Flank Load Carrying Capacity of Case-Hardened Gears", Proceedings of the ASME Design Engineering Technical Conference, 10.
12. König, J., T. Tobie and K. Stahl. 2017, "Optimized flank load carrying capacity II," Load capacity of shot peened and superfinished gear flanks under considerations of the case properties and the lubrication condition (in German)," Project Nr. 521 II (AiF-Nr. 17145), Final report, FVA-magazine Nr. 1245, Frankfurt am Main.
13. Schwienbacher, S., B. Wolter, T. Tobie, K. Stahl, B.-R Höhn, B.-R. and M. Kröning. 2007, „Case properties - gear flank." Investigation and characterization of case parameters and properties and their influence on the flank load carrying capacity of case-hardened, grinded gears (in German)," Porject Nr. 453, Final report, FVA-magazine Nr. 830, Frankfurt am Main.
14. Tobie, T. and P. Matt. 2012, "Recommendations for the Standardization of Load Capacity Tests on Hardened and Tempered Cylindrical Gears," FVA 563/I. Forschungsvereinigung Antriebstechnik e.V. (FVA), Frankfurt am Main.
15. Townsend, D. P. and E.V. Zaretsky. 1982, "Effect of Shot Peening on Surface Fatigue Life of Carburized and Hardened AIS1 9310 Spur Gears," NASA Technical Paper, 2047.
16. Winkelmann, L., O. El-Saeed and M. Bell. 2009, "The Effect of Superfinishing on Gear Micropitting," *Gear Technology*, pp.60–65.
17. [17] Zhang, J. and B.A. Shaw. 2011, "The Effect of Superfinishing on the Contact Fatigue of Case Carburized Gears," *Applied Mechanics and Materials*, 86, pp.348–351

Dominik Kratzer is since 2017 a Research Associate at the FZG Gear Research Centre of the Technical University of Munich. He graduated from the Technical University of Munich with a master's degree in mechanical engineering. His research focuses on the impact of surface finishing processes and material treatments on the load-carrying capacity of gears.

Dr.-Ing. Johannes Koenig studied (2006–2012) Mechanical Engineering at the Technical University of Munich (TUM). From 2012 to 2019 he worked as Research Associate, Team Leader "Materials and Processing" Department "Load Carrying Capacity of Gears" at the Gear Research Centre (FZG), Techncal University of Munich (TUM). He received his PhD in 2020. He currently is an Engineer in the Gear Development Department (Corporate R&D), focusing on Plastic Gear Design & Strength Calculation for ZF Friedrichshafen AG, Friedrichshafen, Germany.

Dr.-Ing. Thomas Tobie studied mechanical engineering at the Technical University of Munich (TUM), Germany. Today he is head of the Load Carrying Capacity of Cylindrical Gears department at the Gear Research Centre (FZG), where he specializes in gear materials, heat treatment, gear lubricants and gear load carrying capacity research. Concurrently, Tobie brings to that work a particular focus on all relevant gear failure modes such as tooth root breakage, pitting, micropitting and wear, as well as sub-surface-initiated fatigue failures.

Prof. Dr.-Ing. Karsten Stahl has since 2011 been Full Professor, Institute for Machine Elements, Technical University of Munich, and the Director Gear Research Centre (FZG). He studied at the Technical University of Munich (TUM) beginning in 1989, with a focus on design and development, receiving his Final Mechanical Engineering Degree (Dr.-Ing) there in 1994. In 2001, he received his Doctorate TUM with the topic: Pitting Resistance of Carburized Spur and Helical Gears. Among his responsibilities during his Professorship: 2009–2010 — Head of Advanced Engineering and Innovation Management, Powertrain and Driving Dynamic Systems, BMW Group, Munich; 2007–2009 — Head of Validation Driving Dynamics and Powertrain, BMW Group, Oxford, UK; 2006–2007 — Head of Quality and QMT MINI Transmission, MINI Plant, BMW Group, Oxford, UK; 2003–2006 — Head of Prototyping, Gear Technology and Methods, BMW Group, Dingolfing; 2001–2003 — Development Engineer in Gear Production, BMW Group, Dingolfing; and 1994–2000 — Scientific Research Assistant (Ph.D. candidate) at Gear Research Centre (FZG), TUM. Prominent among his Professional Activities: Since 2020 DFG: Member of Review Board 402-01; 2016–2018 AiF: Member of Review Board 4. His many honors and awards include (2019) VDMA Faculty Teaching Concept Award, "Bestes Maschinenhaus"; (2019) VDMA Faculty Teaching Concept Award; and (2019) Student Award "Goldene Lehre," Best course of lectures in MW-Bachelor; and (2005) VDI Ring of Honors Award; he has chaired and participated in numerous international conferences, particularly for VDI Gearing Conferences. Stahl's Editorial and many other activities (too numerous to list all here) include: Springer-Nature: Forschung im Ingenieurwesen, journal, Editor in Chief ASME: Journal of Vibration and Acoustics (JVA), Associate Editor Inderscience: International Journal of Powertrains (IJPT), Member of the Editorial Board EDP Sciences: International Journal of Mechanics & Industry, and Editor Tecniche Nuove: Organi di Trasmissione.